Journal of Applied Physics | ARTICLE | pubs.aip.org/aip/jap

Improving electrical contact of vertically aligned carbon nanotubes with bonding metals in thermocompression bonding through oxygen plasma treatment

Cite as: J. Appl. Phys. **138**, 105303 (2025); doi: 10.1063/5.0283506
Submitted: 1 June 2025 · Accepted: 22 August 2025 ·
Published Online: 8 September 2025

View Online

Export Citation

CrossMark

Jianping Zou,[1] Rongtao Jiang,[1,2] Chong Wei Tan,[3] Dominique Baillargeat,[4] Philippe Coquet,[1,5] and Beng Kang Tay[1,2,a)]

AFFILIATIONS

[1]CINTRA IRL 3288, CNRS NTU THALES, Nanyang Technological University, Singapore 637553
[2]Centre for Micro- and Nano-Electronics, School of Electrical and Electronic Engineering, Nanyang Technological University, Singapore 639798
[3]NTI-NTU Corporate Laboratory, Nanyang Technological University, Singapore 637662
[4]CNRS@CREATE Ltd, 1 CREATE Way, CREATE Tower, Singapore 138602
[5]Institut d'Electronique, de Microélectronique et de Nanotechnologie, IEMN, University of Lille, UMR 8520, F-59000 Lille, France

[a)]**Author to whom correspondence should be addressed:** ebktay@ntu.edu.sg

ABSTRACT

Vertically aligned carbon nanotubes (VACNTs) are being widely studied due to their exceptional mechanical, electrical, and thermal properties. The application of thermocompression bonding (TCB) technique has positioned VACNTs as promising candidates for 3D heterogeneous integration, interconnects, and nanopackaging. However, challenges arise from a CNT-cluster layer covering the top surface of the as-grown VACNTs, adversely affecting wettability and electrical contact between the VACNTs and the bonding metals used in the TCB process. To mitigate this issue, we propose using oxygen plasma reactive ion etching (RIE) to treat the top and/or bottom surfaces of the VACNTs. Scanning electron microscopy and Raman spectroscopy characterizations confirm the successful removal of the CNT-cluster layer from the top surface following the RIE treatment, and excessive RIE treatment may cause partial damage to the graphitic structures of the VACNT surface. Direct-current measurements on fabricated VACNT wall π-bridge structures further validate the enhancement in electrical contact between the top surface-treated VACNTs and the bonding metals. This improvement is attributed to the effective removal of the CNT-cluster layer and the relative minimal damage to the graphitic structures, particularly in comparison to the bottom surface-treated VACNTs.

© 2025 Author(s). All article content, except where otherwise noted, is licensed under a Creative Commons Attribution-NonCommercial-NoDerivs 4.0 International (CC BY-NC-ND) license (https://creativecommons.org/licenses/by-nc-nd/4.0/). https://doi.org/10.1063/5.0283506

I. INTRODUCTION

Multi-walled metallic vertically aligned carbon nanotubes (VACNTs) exhibit significant potential for diverse applications, especially in electronic devices and circuits, attributed to their remarkable electrical, thermal, and mechanical properties.[1–3] However, the integration of VACNTs into conventional circuits poses challenges, primarily because their chemical vapor deposition (CVD) synthesis requires high temperatures (typically exceeding 700 °C),[4] which are incompatible with integrated circuit (IC) manufacturing processes. Additionally, the weak adhesion of VACNTs to growth substrates leads to issues with poor device reliability and conductive properties. To address these obstacles, transfer or printing techniques have been proposed to facilitate the transfer of VACNTs from their growth substrates onto target electronic substrates. Nevertheless, challenges remain, including difficulties in precise positioning and maintaining vertical alignment with wet

© Author(s) 2025

chemical methods, as well as concerns regarding high electrical resistance and low repeatability when using physical approaches.[5–7]

A recently developed low-temperature VACNTs transfer technology,[8,9] based on the thermocompression bonding (TCB) process, effectively decouples high-temperature VACNT growth from low-temperature VACNT integration. This advancement enables VACNTs to be transferred from growth substrates to a variety of target substrates at IC-compatible temperature (below 300 °C). Additionally, during the TCB process, the interfacial diffusion of bonding metal (e.g., Au) atoms, facilitated by the concurrent application of heat and force, enhances the adhesion properties of the bonding metal to the metal-coated VACNTs, resulting in improved adhesion of the transferred VACNTs onto host substrates in comparison to the adhesion exhibited by as-grown VACNTs. This enhancement significantly boosts the reliability and conductive properties of VACNT-based devices. These competitive advantages position the TCB-based low-temperature VACNTs transfer technology as highly promising for applications in 3D heterogeneous integrations, nanopackaging, interconnects, and high-frequency devices.[10–12] However, it is important to note that as-grown VACNTs often exhibit poor wettability with metals, primarily attributable to the presence of a CNT-cluster layer on the top of the VACNT forest (see Fig. 1). The formation of this CNT-cluster layer occurs during the initial stages of the CVD-growth process,[13–17] during which the CNTs self-organize to develop a cluster layer that shapes the morphology of the entire forest and enables subsequent vertical growth of the CNTs. This CNT-cluster layer comprises randomly distributed, twisted, and intertwined CNTs that aggregate into small clusters (highlighted by the red circles in Fig. 1), presenting significant challenges in achieving reliable bonding strength and ensuring substantial electrical contact between the VACNTs and the bonding metals during the TCB process.

To tackle this issue, we proposed utilizing oxygen (O_2) plasma reactive ion etching (RIE) to treat the top and/or bottom surfaces of VACNTs, effectively removing the CNT-cluster layer prior to the TCB process. We performed four types of RIE treatments: treatment of only the top surface, treatment of only the bottom surface, treatment of both surfaces, and a control group with no treatment. Scanning electron microscopy (SEM) characterization confirmed the effective removal of the CNT-cluster layer following the top-surface RIE treatment. Raman spectroscopy indicated that excessive etching may cause partial damage to the graphitic structures of the VACNT surfaces. With the CNT-cluster layer eliminated from the top surface, the exposure of the VACNT tips facilitates enhanced wettability and electrical contact with the bonding metals. Additionally, direct-current (DC) measurements conducted on VACNT wall π-bridge structures fabricated using the TCB process with the four different RIE treatments further validated the improved electrical contact between the top surface-treated VACNTs and the bonding metals.

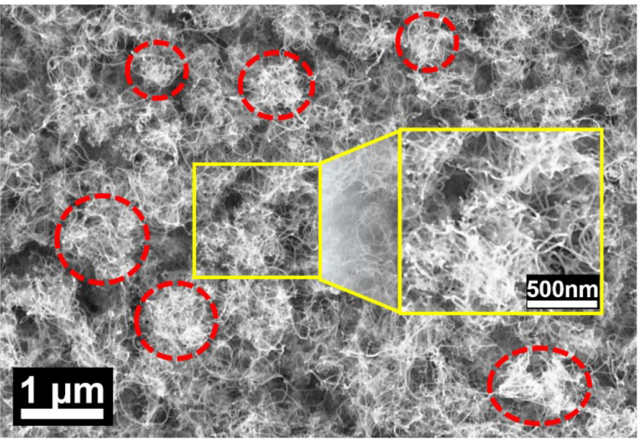

FIG. 1. SEM image of the top surface morphology of an as-grown VACNT forest. (The image was taken from a top view of the surface without any tilt.)

II. EXPERIMENTAL METHODS

A. VACNT arrays preparation

The desired VACNT patterns were initially prepared using lithography on a Si substrate with 270 nm thick thermally grown SiO_2. Subsequently, a catalyst layer consisting of a 1.1 nm thick Fe film and a 10 nm thick Al_2O_3 diffusion barrier was deposited onto the pre-patterned substrate using electron beam (e-beam) physical vapor deposition (PVD). A lift-off process was then implemented to form the patterned catalyst layer. Following this, multi-walled VACNT arrays were synthesized at a temperature of 750 °C using Ar and H_2 as carrier gases and C_2H_4 as the carbon source, within a commercial CVD system (FirstNano Easytube® 3000). To facilitate the detachment of the VACNT arrays from the Si substrate during the subsequent TCB-based VACNT transfer process, a water vapor etching procedure was performed after the VACNT growth to weaken the adhesion of the VACNTs on the Si substrate.[12] The height of the VACNTs can be adjusted by varying the growth duration.

B. O_2 plasma RIE treatment of the top and/or bottom surface of VACNT arrays

The top surface of the as-grown VACNT arrays underwent treatment using the O_2 plasma RIE. The radio frequency (RF) power was set at 100 W, and the flow rate of O_2 was maintained at 30 SCCM. Different RIE durations of 15, 30, and 45 s were chosen for the subsequent characterization of the surface morphology evolution of the treated VACNTs. During the TCB transfer process, the as-grown VACNT arrays were transferred onto new target substrates, with the top surface securely bonded to the target substrates. In contrast, the original bottom surface of the VACNT arrays remained exposed to the air after the TCB transfer process. In a manner similar to that of the original top surface, RIE treatments were applied to the exposed bottom surface under the same processing conditions.

C. SEM and Raman characterizations of the O_2 plasma-treated VACNTs

The influence of the O_2 plasma RIE treatment on the VACNT surface morphology was examined using SEM, and Raman

© Author(s) 2025

spectroscopy was utilized to investigate the crystallinity and quality of the VACNTs following the RIE treatment.

D. VACNT wall π-Bridge structures

To validate the enhanced electrical contact between the O_2 plasma-treated VACNTs and the bonding metals, a VACNT wall π-bridge structure [Fig. 2(a)] was designed for DC measurements. This π-bridge structure was constructed utilizing the TCB-based VACNT transfer technology. Initially, two VACNT walls measuring 5 mm in length (L), 0.25 mm in width (W), and 0.5 mm in height (H) were grown on a Si substrate, followed by the O_2 plasma RIE treatment of the top surface of the VACNT walls [Fig. 2(b)]. A bonding metal layer comprising Ti/Au (30 nm/150 nm) was then deposited on the top surface of the RIE-treated VACNT walls [Fig. 2(c)]. Subsequently, an Au–Au TCB process was executed using a flip-chip bonder at a temperature of 300 °C [Fig. 2(d)]. This step involved bonding the Si substrate with Au-coated VACNT walls to another Si substrate (referred to as "top cover") with a pre-coated Ti/Au layer. Thanks to the stronger bonding strength between the VACNT walls and the Si top cover, the VACNT walls were transferred onto the top cover by mechanically detaching them from the original Si growth substrate [Fig. 2(e)]. After the initial TCB transfer process, the original bottom surface of the VACNT walls was revealed. This bottom surface underwent a treatment with O_2 plasma [Fig. 2(e)], followed by an additional deposition of Ti/Au [Fig. 2(f)]. Finally, another TCB process was performed to bond the top cover with the transferred VACNT walls to a Si bottom substrate with two separate Au electrodes [Fig. 2(g)]. Each of the two transferred VACNT walls made contact with one of the two Au electrodes, thereby forming the π-bridge structure. Figure 3(a) shows the Au-coated Si top cover with the two VACNT walls after the initial TCB transfer process. In Fig. 3(b), the fully constructed π-bridge structure is shown, with the VACNT walls positioned between the inverted top cover and the bottom substrate, which includes two separate Au electrodes. To evaluate the impact of the RIE treatment on the electrical contact quality of the VACNT wall π-bridge structure, four distinct RIE treatments were implemented to construct the π-bridge structures. These included treating only the top surface, treating only the bottom surface, treating both surfaces, and a control group without any treatment.

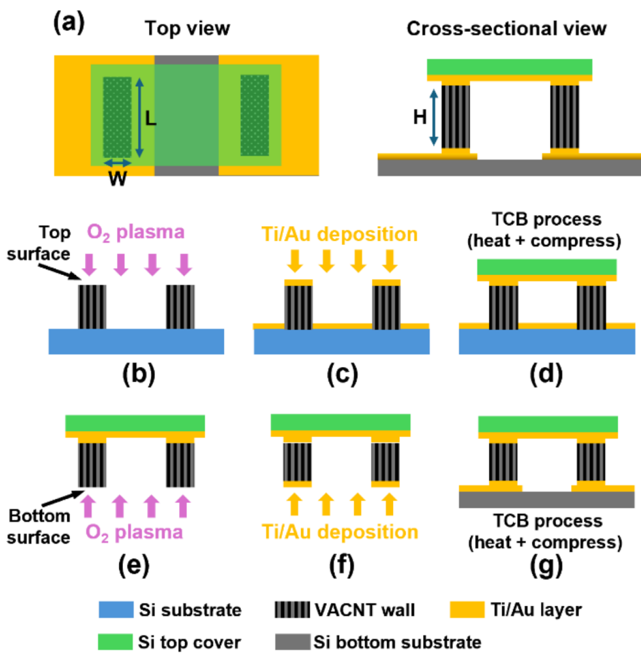

FIG. 2. VACNT wall π-bridge structure. (a) Top and cross-sectional views of the structure. (b) VACNT walls grown on a Si substrate, followed by top surface treatment using O2 plasma. (c) Ti/Au layer deposited on the VACNT walls. (d) TCB process for bonding of the VACNT walls to a Si top cover. (e) O2 plasma treatment for the bottom surface of the VACNT walls transferred onto the top cover. (f) Ti/Au layer deposited on the transferred VACNT walls. (g) TCB process for bonding the transferred VACNT walls to a Si bottom substrate to complete the π-bridge structure.

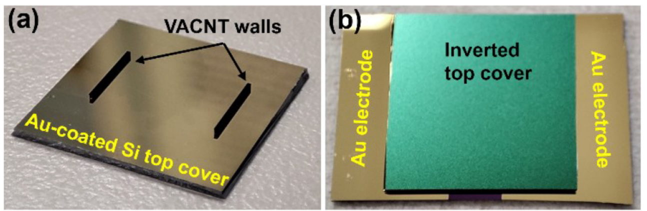

FIG. 3. (a) Two VACNT walls transferred on the Au-coated Si top cover after the initial TCB process. (b) The completed VACNT wall π-bridge structure device.

III. RESULTS AND DISSCUSION

During O_2 plasma RIE treatment on a densely packed film of VACNTs, it is reasonable to believe that the upper side of the VACNTs, which is directly exposed to the plasma, serves as a barrier, thereby shielding the lower portion of the VACNTs from the etching process. Consequently, the RIE-induced modifications that occur to the VACNTs are mainly localized to the top surface. The SEM images shown in Fig. 4 present the top surface morphology of the VACNT walls subjected to varying durations of RIE treatment. For SEM analysis, the sample surface was inclined at an angle of 15°, with imaging consistently performed at a magnification of 3000× to enable a comparative assessment. Prior to the RIE treatment, the as-grown VACNT top surface was observed to be covered by a CNT-cluster layer, as shown in Fig. 4(a) (similar to Fig. 1). Following a 15 s exposure to O_2 plasma, this CNT-cluster layer was almost entirely removed compared to the as-grown VACNT top surface [Fig. 4(a)], revealing the underlying VACNT tip bundles [Fig. 4(b)] while preserving the integrity of the vertically aligned structure. Extending the RIE duration to 30 s resulted in further exposure of the VACNT tip bundles to the O_2 plasma. Consequently, these VACNT tip bundles exhibited signs of partial etching, attributable to the different VACNT tip heights and the enhanced reactivity of the nanotube tips relative to that of the

© Author(s) 2025

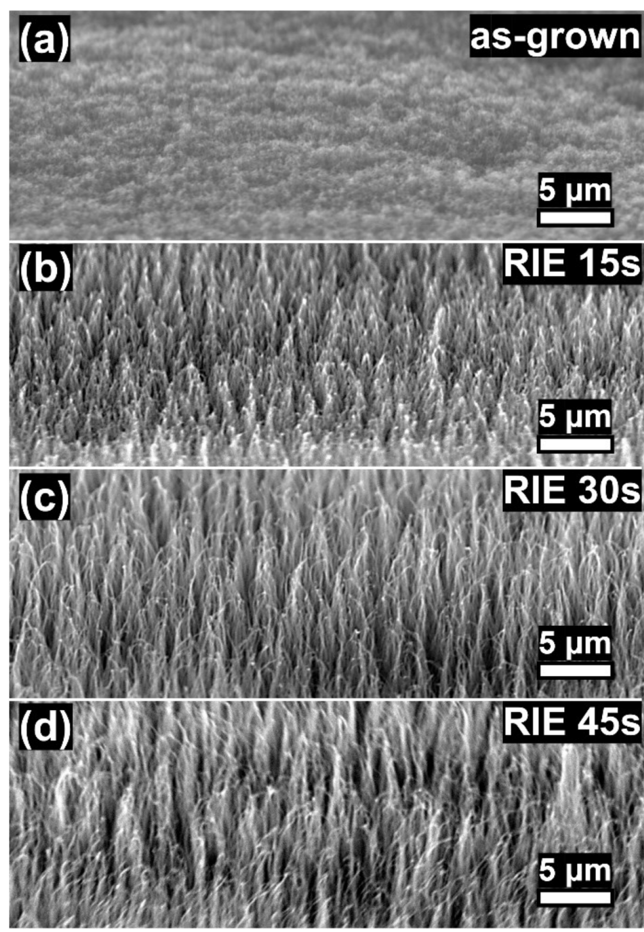

FIG. 4. SEM images of the top surface morphology of (a) the as-grown, (b) 15, (c) 30, and (d) 45 s RIE-treated VACNT walls. (The sample surface was tilted by 15° for SEM observations.)

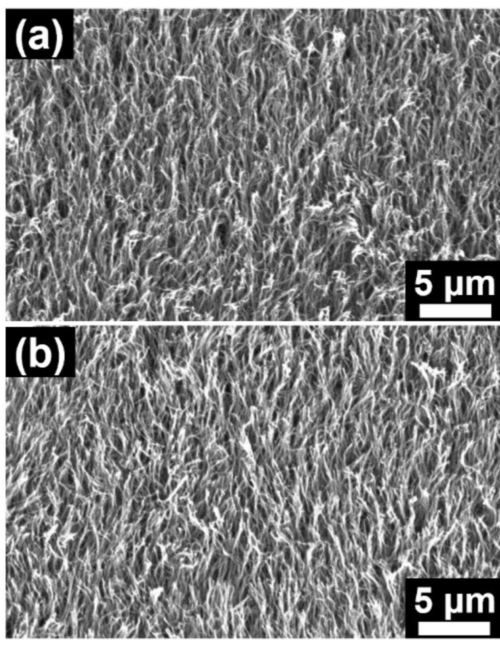

FIG. 5. SEM image of (a) the exposed bottom surface of the VACNT walls after the initial TCB process and (b) the bottom surface after 15 s RIE treatment. (The sample surface was tilted by 20° for SEM observations.)

tubular walls.[18–20] As a result, the VACNT tip bundles that underwent partial etching displayed a markedly sparser surface morphology [Fig. 4(c)] when compared to the treatment of 15 s [Fig. 4(b)]. Further increases in the RIE time to 45 s did not produce significant alterations in the surface morphology [Fig. 4(d)] compared to the 30 s RIE treatment [Fig. 4(c)] due to the modest etching process and robust vertically aligned structure of CNTs. Based on the SEM characterization results, 15 s RIE treatment was deemed optimal and selected for removing the CNT-cluster layer while preserving the structural integrity of the VACNTs for subsequent fabrication of π-bridge structures.

During the fabrication process of VACNT wall π-bridge structures (as depicted in Fig. 2), the VACNT walls were transferred onto the Si top cover following the initial TCB process [Fig. 2(d)]. In this step, the VACNT top surface was securely bonded to the top cover, revealing the original VACNT bottom surface [Fig. 2(e)]. In contrast to the top surface, the bottom surface [Fig. 5(a)] displayed a more uniformly distributed arrangement of VACNT tips, lacking the pronounced twisted and intertwined morphologies observed previously in the top surface (Fig. 1). Additionally, the 15 s RIE treatment applied to the VACNT bottom surface did not significantly alter its surface morphology, as shown in Fig. 5(b).

To further investigate the impact of the RIE treatment on the crystallinity and quality of the VACNTs, Raman spectroscopy was employed, with spectra for both the as-grown and RIE-treated VACNTs depicted in Fig. 6(a). All spectra mainly exhibited two peaks at approximately 1345 cm^{-1} (D band) and 1579 cm^{-1} (G band), which correspond to disordered and graphitic carbon signals, respectively.[21–23] Notably, with increased RIE time from 15 to 45 s, a slight broadening of the G band was observed, attributable to the excessive etching of the graphitic structures near the VACNT tips [as illustrated in Fig. 4(c)]. The intensity ratio of the D peak relative to the G peak (I_D/I_G) can be utilized to assess the degree of disorder within the sample.[22] These disordered structures could be vacancies, extra adsorbed carbon atoms, imperfect nanotube edges, and grain boundaries between small graphitic domains. Figure 6(b) illustrates the relationship between the I_D/I_G and the duration of RIE treatment, revealing a gradual increase in this ratio as RIE time extends. This trend is consistent with excessive etching-induced damage to the graphitic structures near the VACNT tips, which correlates with a higher degree of disorder within the VACNT structure.

To assess the impact of O_2 plasma RIE treatment on the electrical contact characteristics between VACNTs and the bonding

© Author(s) 2025

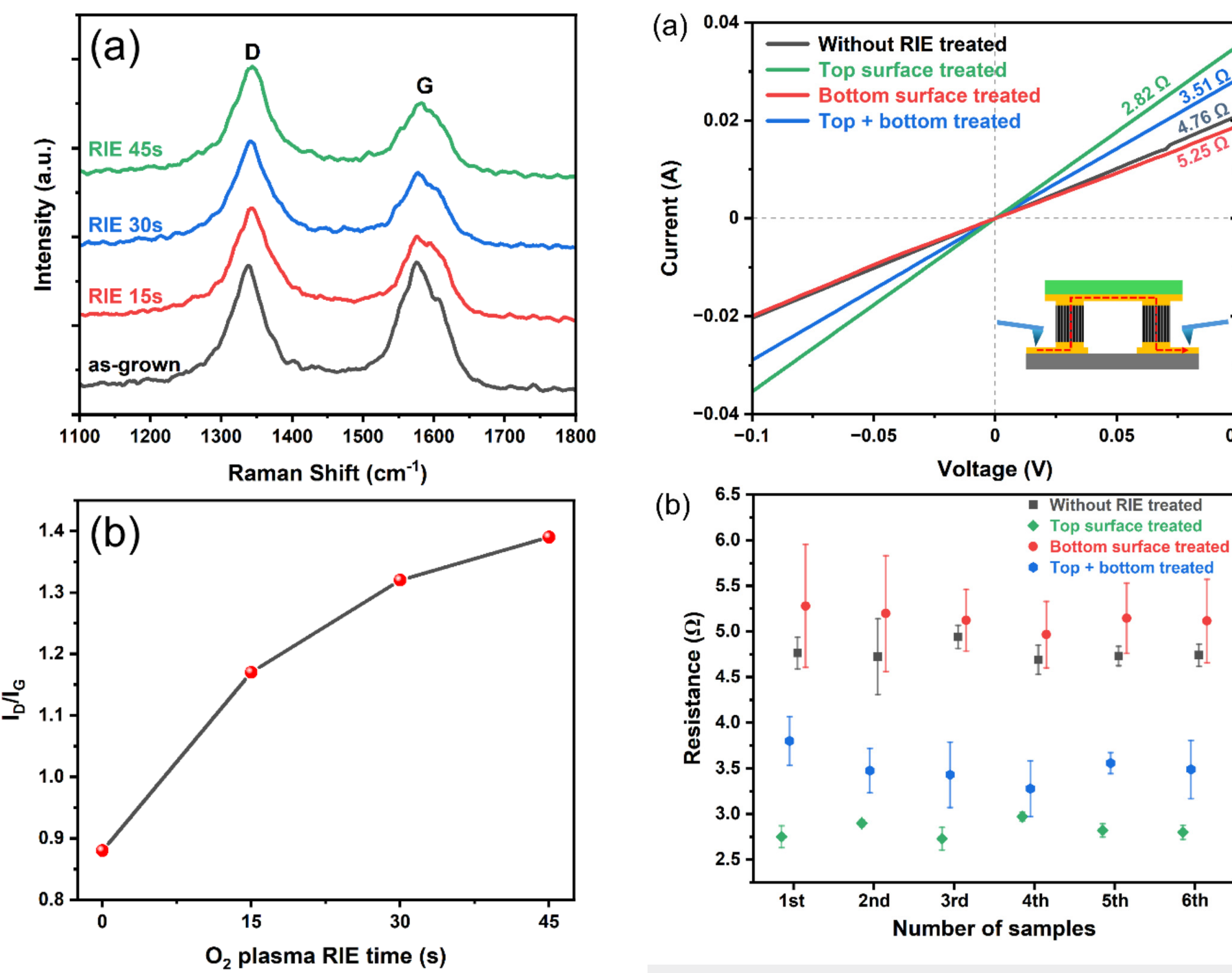

FIG. 6. (a) Raman spectra of the as-grown, and 15, 30, and 45 s O2 plasma RIE-treated VACNTs. (b) The intensity ratio (ID/IG) of the D band to the G band as a function of the RIE duration. (Raman measurements were performed on a representative VACNT sample.)

FIG. 7. (a) The measured I–V characteristics of four representative VACNT wall π-bridge structures, each corresponding to one of the four distinct RIE treatments. (b) The statistical comparison of both the average resistance values and the standard deviations for six samples corresponding to each type of RIE treatment.

metals employed in the TCB process, DC measurements were systematically conducted on the fabricated VACNT wall π-bridge structures with four different RIE treatments to VACNTs (i.e., only the top surface treatment, only the bottom surface treatment, both surfaces treatment, and no treatment at all). For all RIE treatments, a duration of 15 s was chosen for effectively removing the CNT-cluster layer from the top surface while preserving the crystalline structural integrity of the VACNTs. The DC measurement schematic with the structure is illustrated in the inset of Fig. 7(a). A voltage was applied across two probes for measuring the current traversing through the structure (as indicated by the red dashed line in the inset).

For each type of RIE treatment, a total of six samples were measured. Within each sample, ten different probe locations were selected for testing to generate ten sets of current–voltage (I–V) data for subsequent statistical analysis. Figure 7(a) showcases the measured I–V characteristics of four representative samples, each corresponding to one of the four distinct RIE treatments. The I–V responses of all four samples demonstrated a linear relationship, indicative of the ohmic nature of the bonding interface between the VACNTs and the Au bonding layer. The calculated resistance of the top surface-treated sample is $2.82\,\Omega \pm 0.091\,\Omega$, markedly less than that ($4.76\,\Omega \pm 0.089\,\Omega$) of the sample without RIE treatment. This significant reduction in resistance is primarily attributed to the RIE treatment-induced effective removal of the CNT-cluster

© Author(s) 2025

layer, which enhances the wettability of the VACNT top surface with the Au bonding layer, thus contributing to an improved electrical contact. It is worth noting that the calculated resistance ($5.25\,\Omega \pm 0.142\,\Omega$) of the bottom surface-treated sample is not significantly lower than that ($4.76\,\Omega$) of the untreated sample; in fact, it is slightly higher. This is primarily due to the fact that the VACNT bottom surface is not covered by the CNT-cluster layer typically found on the VACNT top surface. Therefore, the VACNT bottom surface was directly exposed to the O_2 plasma during the RIE treatment, which leads to the partial destruction of the VACNT graphitic structures on the bottom surface, degrading the electrical contact between the VACNT bottom surface and the Au bonding layer. This degraded electrical contact caused a slightly increased resistance in the bottom surface-treated sample compared to the untreated sample. Additionally, the sample that underwent both top and bottom surface treatments displayed a resistance of $3.51 \pm 0.103\,\Omega$. Under the dual effects of removing the CNT-cluster layer from the top surface and the partial destruction of the graphitic structure on the bottom surface brought about by the RIE treatment on both surfaces, the resistance ($3.51\,\Omega$) of both the surface-treated sample is significantly smaller than $4.76\,\Omega$ found in the untreated sample, while also lying between that ($2.82\,\Omega$) of the top surface-treated sample and that ($5.25\,\Omega$) of the bottom surface-treated sample.

Figure 7(b) presents a statistical comparison of both the average resistance values and the standard deviations for six samples corresponding to each type of RIE treatment. The top surface-treated samples demonstrated not only lower resistance but also a smaller standard deviation compared to the other three treated counterparts. This improvement is attributed to the effective removal of the CNT-cluster layer and the relatively minimal damage to the graphitic structures, particularly in comparison to the bottom surface treatment.

While the resistance reduction and improved consistency were herein demonstrated at millimeter-scale contact dimensions, this research validates the fundamental efficacy of the RIE treatment in enhancing the electrical contact between the VACNTs and the Au bonding layer. To effectively incorporate VACNTs into integrated circuit manufacturing processes, further studies focused on downscaling contact dimensions would be beneficial. This endeavor will involve the fabrication and characterization of multiple VACNT contact lines with varying feature sizes on a single wafer, facilitating a comprehensive exploration of the RIE process window at micro- and nano-scales. Such investigations present additional complexities, including the development of nano-scale patterning techniques for both the VACNTs and bonding metals, optimizing lithography patterns for finer features, and adapting electrical probing methods for sub-micrometer contacts. These considerations warrant a dedicated future investigation.

IV. CONCLUSIONS

An O_2 plasma RIE process was employed to treat the top and/or bottom surfaces of VACNTs to improve the electrical contact between the VACNTs and the Au bonding layer used in the TCB transfer process. SEM characterizations revealed that the CNT-cluster layer covering the top surface of the freshly grown VACNTs can be effectively removed through RIE treatment. Raman spectroscopy characterizations confirmed that excessive RIE treatment may lead to partial damage of the graphitic structures of the VACNT surface. To evaluate the impact of the RIE treatment, the VACNT wall π-bridge structures were designed and fabricated with four different RIE treatments for DC measurements. The results indicated that the top surface-treated samples exhibited lower resistance, attributed to improved wettability and electrical contact between the VACNTs and the Au bonding layer. The successful implementation and validation of this optimized O_2 plasma RIE treatment mark a major advancement in VACNT technology. By addressing a critical bottleneck in their integration, the challenge of establishing robust and reliable electrical contact, this research significantly enhances the viability and potential of VACNTs when integrating them with electronic substrates, paving the way for their widespread adoption in transformative applications, including high-density 3D heterogeneous integration, advanced nanopackaging solutions, and high-performance interconnect technologies. Ultimately, the method not only enhances the intrinsic capabilities of VACNTs but also provides valuable insights into precision surface engineering for other advanced nanomaterials, thereby contributing significantly to the ongoing innovation and future trajectory of the electronics community.

ACKNOWLEDGMENTS

This research was supported by the National Research Foundation, Singapore and Infocomm Media Development Authority under its Future Communications Research & Development Programme [No. FCP-CNRS-RG-2022-022 (REQ0396559)]. The authors would also like to thank Professor H. T. Teo for the provision of the CVD system used in this work.

AUTHOR DECLARATIONS

Conflict of Interest

The authors have no conflicts to disclose.

Author Contributions

Jianping Zou: Conceptualization (equal); Data curation (lead); Formal analysis (equal); Investigation (equal); Methodology (equal); Validation (lead); Visualization (equal); Writing – original draft (equal); Writing – review & editing (equal). **Rongtao Jiang:** Data curation (equal); Formal analysis (supporting); Methodology (supporting); Writing – original draft (supporting); Writing – review & editing (supporting). **Chong Wei Tan:** Conceptualization (supporting); Formal analysis (supporting); Methodology (supporting); Writing – review & editing (supporting). **Dominique Baillargeat:** Funding acquisition (supporting); Project administration (supporting); Resources (supporting); Writing – review & editing (supporting). **Philippe Coquet:** Methodology (supporting); Resources (supporting); Supervision (supporting); Writing – review & editing (supporting). **Beng Kang Tay:** Conceptualization (lead); Funding acquisition (lead); Project administration (lead); Resources (lead); Supervision (lead); Writing – original draft (lead); Writing – review & editing (lead).

© Author(s) 2025

DATA AVAILABILITY

The data that support the findings of this study are available from the corresponding author upon reasonable request.

REFERENCES

[1]N. Chiodarelli, S. Masahito, Y. Kashiwagi, Y. Li, K. Arstila, O. Richard, D. J. Cott, M. Heyns, S. De Gendt, G. Groeseneken, and P. M. Vereecken, "Measuring the electrical resistivity and contact resistance of vertical carbon nanotube bundles for application as interconnects," Nanotechnology **22**(8), 085302 (2011).

[2]R. Saito, G. Dresselhaus, and M. S. Dresselhaus, *Physical Properties of Carbon Nanotubes* (Imperial College Press, 1998).

[3]Z. Hu and X. Lu, "Mechanical properties of carbon nanotubes and graphene," in *Carbon Nanotubes and Graphene*, 2nd ed., edited by K. Tanaka and S. Iijima (Elsevier, Oxford, 2014), Chap. 8, pp. 165–200.

[4]P. Avouris, J. Appenzeller, R. Martel, and S. J. Wind, "Carbon nanotube electronics," Proc. IEEE **91**(11), 1772–1784 (2003).

[5]M. A. Meitl, Y. Zhou, A. Gaur, S. Jeon, M. L. Usrey, M. S. Strano, and J. A. Rogers, "Solution casting and transfer printing single-walled carbon nanotube films," Nano Lett. **4**(9), 1643–1647 (2004).

[6]A. Kumar, V. L. Pushparaj, S. Kar, O. Nalamasu, P. M. Ajayan, and R. Baskaran, "Contact transfer of aligned carbon nanotube arrays onto conducting substrates," Appl. Phys. Lett. **89**(16), 163120 (2006).

[7]F. N. Ishikawa, H. Chang, K. Ryu, P. Chen, A. Badmaev, L. Gomez De Arco, G. Shen, and C. Zhou, "Transparent electronics based on transfer printed aligned carbon nanotubes on rigid and flexible substrates," ACS Nano **3**(1), 73–79 (2009).

[8]J. Wang, P. Coquet, and B. K. Tay, "Nanostructure transfer method," Singapore patent application 10201807403V (29 August 2018).

[9]C. F. Siah, L. Y. X. Lum, J. Wang, S. C. K. Goh, C. W. Tan, L. Hu, P. Coquet, H. Li, C. S. Tan, and B. K. Tay, "Development of a CMOS-compatible carbon nanotube array transfer method," Micromachines **12**(1), 95 (2021).

[10]J.M. de Saxce, P. Roux-Levy, C.F. Siah, J. Wang, B.K. Tay, P. Coquet, and D. Baillargeat, "Millimeter wave carbon nanotube based flip chip coplanar interconnects," in *2020 IEEE 22nd Electronics Packaging Technology Conference (EPTC)* (IEEE, Singapore, 2020), pp. 81–84.

[11]S. Chun Kiat Goh, C. Fei Siah, J. De Saxce, Z. Ng, L. Lynn Shiau, L. Lum Yun Xiang, C. Wei Tan, E. Hang Tong Teo, P. Coquet, D. Baillargeat, and B. Kang Tay, "2.5D technology based on vertically aligned carbon nanotubes for MM-waves passive devices," in *2023 IEEE/MTT-S International Microwave Symposium—IMS 2023* (IEEE, 2023), pp. 767–770.

[12]L. Lum, D. Tan, C. W. Tan, and B. K. Tay, "Electromagnetic crosstalk isolation with transferred vertically aligned carbon nanotube arrays through thermocompression bonding," Carbon **221**, 118943 (2024).

[13]M. F. L. De Volder, D. O. Vidaud, E. R. Meshot, S. Tawfick, and A. John Hart, "Self-similar organization of arrays of individual carbon nanotubes and carbon nanotube micropillars," Microelectron. Eng. **87**(5), 1233–1238 (2010).

[14]H. S. Ahn, N. Sinha, M. Zhang, D. Banerjee, S. Fang, and R. H. Baughman, "Pool boiling experiments on multiwalled carbon nanotube (MWCNT) forests," J. Heat Transfer **128**(12), 1335–1342 (2006).

[15]L. Zhang, Z. Li, Y. Tan, G. Lolli, N. Sakulchaicharoen, F. G. Requejo, B. S. Mun, and D. E. Resasco, "Influence of a top crust of entangled nanotubes on the structure of vertically aligned forests of single-walled carbon nanotubes," Chem. Mater. **18**(23), 5624–5629 (2006).

[16]Y. Li, H. Zhang, Y. Yao, T. Li, Y. Zhang, Q. Li, and Z. Dai, "Transfer of vertically aligned carbon nanotube arrays onto flexible substrates for gecko-inspired dry adhesive application," RSC Adv. **5**(58), 46749–46759 (2015).

[17]M. F. L. De Volder, S. J. Park, S. H. Tawfick, D. O. Vidaud, and A. J. Hart, "Fabrication and electrical integration of robust carbon nanotube micropillars by self-directed elastocapillary densification," J. Micromech. Microeng. **21**(4), 045033 (2011).

[18]S. Huang and L. Dai, "Plasma etching for purification and controlled opening of aligned carbon nanotubes," J. Phys. Chem. B **106**(14), 3543–3545 (2002).

[19]D. T. Colbert, J. Zhang, S. M. McClure, P. Nikolaev, Z. Chen, J. H. Hafner, D. W. Owens, P. G. Kotula, C. B. Carter, J. H. Weaver, A. G. Rinzler, and R. E. Smalley, "Growth and sintering of fullerene nanotubes," Science **266**(5188), 1218–1222 (1994).

[20]P. M. Ajayan, T. W. Ebbesen, T. Ichihashi, S. Iijima, K. Tanigaki, and H. Hiura, "Opening carbon nanotubes with oxygen and implications for filling," Nature **362**(6420), 522–525 (1993).

[21]P. Li, X. Lim, Y. Zhu, T. Yu, C.-K. Ong, Z. Shen, A. T.-S. Wee, and C.-H. Sow, "Tailoring wettability change on aligned and patterned carbon nanotube films for selective assembly," J. Phys. Chem. B **111**(7), 1672–1678 (2007).

[22]A. Jorio, E. H. M. Ferreira, M. V. O. Moutinho, F. Stavale, C. A. Achete, and R. B. Capaz, "Measuring disorder in graphene with the G and D bands," Phys. Status Solidi B **247**(11–12), 2980–2982 (2010).

[23]A. Dychalska, P. Popielarski, W. Franków, K. Fabisiak, K. Paprocki, and M. Szybowicz, "Study of CVD diamond layers with amorphous carbon admixture by Raman scattering spectroscopy," Mater. Sci. **33**(4), 799–805 (2015).

© Author(s) 2025